

Albedo and laser threshold of a diffusive Raman gain medium

A C SELDEN

Department of Physics
University of Zimbabwe
Mount Pleasant MP 167
HARARE Zimbabwe

adrian_selden@yahoo.com

ABSTRACT

The diffuse reflectance (albedo) and transmittance of a Raman random gain medium are calculated via semi-analytic two-stream equations with power-dependent coefficients. The results show good qualitative agreement with the experimental data for barium nitrate powder. A divergence in reflectance at a critical gain is interpreted as the threshold for diffusive Raman laser generation. The dependence of the generation threshold on the scattering parameters is analysed and the feedback effect of Fresnel reflection at the gain boundaries evaluated. The addition of external mirrors, particularly at the pumped surface, significantly reduces the threshold gain.

Keywords: Random laser, Raman scattering, Two-stream equations, Albedo

PACS Nos. 42.55.Ye, 42.55.Zz

Introduction

A number of non-linear optical effects have been observed in random laser media via the enhanced interaction arising from multiple scattering and gain, namely second harmonic generation [1, 2], higher harmonic generation [3], anti-Stokes random lasing [4], up-conversion lasing [5] and surface plasmon enhanced Raman scattering [6] and random lasing [7]. Raman random lasing has been reported in SiC nanorods [8] and the Raman random laser threshold evaluated for a cloud of cold atoms [9]. Raman gain has been observed in barium nitrate powder via enhanced reflectance and transmission gain of a Raman probe [10]. Unlike conventional optically pumped random lasers, which function by optical excitation via the absorption bands, Raman random laser media require no intrinsic absorption, but operate by non-linear conversion of the pump light. As such they are ideally lossless, any residual absorption arising from impurities and surface contamination, thereby enabling the pump flux to reach much greater depths than in optically pumped random lasers. Raman gain observed in mono-crystalline barium nitrate powder has been modelled as a radiative transfer process in a scattering medium with non-uniform gain using Monte Carlo methods, the gain profile being determined from the observed variation of pump intensity with optical depth [10]. The pump radiation penetrates to a depth ~ 2 mm, equivalent to ~ 20 scattering lengths in a layer of randomly packed cubic crystals ~ 0.2 - 0.3 mm in size. A linear analysis of the propagation of light in powdered laser media has previously been made using the Kubelka-Munk two-flux equations with constant coefficients [11] and the dynamics of a 1D random laser modelled using the time-dependent diffusion equation [12]. Diffusion analysis has also been applied to model two-photon absorption in a random medium [13] and the distribution of second harmonic light in porous GaP [2]. Here we describe a semi-analytic two-stream model of diffusive Raman gain in a random medium, which gives good qualitative agreement with experimental data for diffuse Raman reflectance and transmission gain of barium nitrate powder [10]. Having validated the two-stream analysis, we use it to determine the parametric dependence of the albedo and Raman laser threshold on the scattering characteristics of a random gain medium with feedback provided by Fresnel reflection of diffuse light at the gain boundaries [14]. The effect of specularly reflecting boundaries is also analysed [15].

Two-stream analysis

Two-stream theory follows on integrating the radiative transfer equation over the forward and backward hemispheres, leading to a pair of coupled differential equations describing the spatial variation of the forward and backward radiative fluxes F_+ , F_-

$$dF_+/d\tau = \gamma_{11} F_+ - \gamma_{12} F_- - S_+ \quad (1a)$$

$$dF_-/d\tau = \gamma_{21} F_+ - \gamma_{22} F_- + S_- \quad (1b)$$

where γ_{mn} are transport coefficients, S_+ , S_- are source terms and τ is the optical depth [16]. The two-stream equations can be expressed in vector matrix form

$$d\mathbf{F}/d\tau = \mathbf{M}\mathbf{F} + \mathbf{S} \quad (2)$$

where $\mathbf{M}(\gamma)$ is the transfer matrix, $\mathbf{F}(\tau)$ the vector flux and $\mathbf{S}(\tau)$ the vector source. This formalism is readily extended to higher order (multi-stream) analysis [16]. Selection of suitable source terms S_+ , S_- for photons scattered from the collimated probe beam enables calculation of the diffuse transmittance and hemispherical reflectance (albedo) of the scattering medium.

Transfer coefficients and rescaling

The standard Eddington approximation is used for the transport coefficients [16], modified to make the gain explicit [17]

$$\gamma_{11} = \gamma_{22} = \frac{1}{4}[7(1-\gamma) - \varpi(4+3g)] \quad (3a)$$

$$\gamma_{12} = \gamma_{21} = -\frac{1}{4}[(1-\gamma) - \varpi(4-3g)] \quad (3b)$$

with gain parameter $\gamma = \gamma_R \lambda_s$; the Raman gain coefficient $\gamma_R(\tau) = \Gamma_R F_p(\tau)$, where Γ_R is the Raman parameter and $F_p(\tau)$ the diffuse pump flux, λ_s is the scattering length, ϖ the particle scattering albedo and g is the scattering asymmetry: $g = \frac{1}{2} \int \bar{p}(\mu_s) \mu_s d\mu_s$, where $\bar{p}(\mu_s)$ is the azimuthally averaged phase function, $\mu_s = \cos \theta_s$ and θ_s is the

scattering angle ($g \Rightarrow 1$ for forward scattering). The forward biased phase function is approximated by a simple two-term expression

$$\bar{p}(\mu_s) = 2\beta\delta|1-\mu_s| + (1-\beta)[1+3b_1\mu_s] \quad (4)$$

the δ -function representing the narrow diffraction peak containing a fraction β of the total scattered energy, the linear term approximating the wide angle diffuse scattering distribution. The use of a δ -function enables rescaling of the optical depth as $d\tau' = (1-\beta\varpi)d\tau$ and albedo as $\varpi' = \varpi(1-\beta)/(1-\beta\varpi)$ and reduces the phase function to the linear term [16]. For a Henyey-Greenstein phase function with asymmetry g we have $\beta = g^2$ and $b_1 = g/(1+g)$ [16]. The rescaled transfer coefficients are

$$\gamma'_{11} = \gamma'_{22} = \frac{1}{4}[7(1-\gamma')-\varpi'(4+3b_1)] \quad (5a)$$

$$\gamma'_{12} = \gamma'_{21} = -\frac{1}{4}[(1-\gamma')-\varpi'(4-3b_1)] \quad (5b)$$

where $\gamma' = \gamma/(1-\beta\varpi)$. The source terms for the diffuse Raman radiation scattered from the attenuated probe flux $f_p(\tau)$ and their rescaled forms are

$$S_+ = \varpi\gamma_3 f_p(\tau) \Rightarrow S'_+ = \varpi'\gamma'_3 f_p(\tau') \quad (6a)$$

$$S_- = \varpi(1-\gamma_3) f_p(\tau) \Rightarrow S'_- = \varpi'(1-\gamma'_3) f_p(\tau') \quad (6b)$$

where $f_p(\tau) = f_p(0)\exp(-\tau/\mu_0)$, μ_0 is the cosine of the angle between the inward surface normal and the incident beam ($\mu_0 = 1$ for normal incidence) and [16]

$$\gamma_3 = \frac{1}{4}[2-3g\mu_0] \Rightarrow \gamma'_3 = \frac{1}{4}[2-3b_1\mu_0] \quad (7)$$

The rescaled two-stream equations are applied to calculate the diffuse reflectance and transmittance of the Raman random gain medium. The corresponding diffusion equation is derived in the Appendix.

Albedo equation

Defining $F_- = RF_+$ and substituting in eqns 1(a, b) yields the source-free albedo equation (with $S_+, S_- = 0$)

$$dR/d\tau = \gamma_{21} - (\gamma_{11} + \gamma_{22})R + \gamma_{12}R^2 \quad (8)$$

where $R(\tau) = F_-(\tau)/F_+(\tau)$ is the diffuse reflectance function. The steady state solution is matched to the boundary reflectances $R(0) = R_0$ and $R(\tau_1) = 1/R_1$ [17]. Inserting the transfer coefficients defined in eqns 4(a, b) we have

$$dR/d\tau + 2\gamma_{11}(\tau)R = \gamma_{12}(\tau)(1+R^2) \quad (9)$$

With the substitution $R = \tan \pi u/2$ this reduces to [17]

$$du/d\tau = \gamma_{12}(\tau) - \gamma_{11}(\tau) \sin \pi u \quad (10)$$

which can be used to determine the generation threshold for a particular configuration of the Raman gain medium with specified (reflecting) boundaries.

Raman albedo

Two-stream calculations were carried out for collimated pump and probe beams incident on barium nitrate powder samples sandwiched between glass plates, for sample depths in the range $d = 10-100\lambda_s$ [10]. The fluxes of amplified Raman radiation were determined by equating the hemispherical flux leaving a boundary with the specularly reflected incident flux: $F_-(0) = R_b F_+(0)$ and $F_+(\tau_0) = R_b F_-(\tau_0)$, where R_b is the Fresnel reflection coefficient for diffuse radiation incident at a dielectric surface [14] and τ_0 is the optical depth of the powder. This condition is satisfied simultaneously at both boundaries for a specific value of the radiative flux, enabling the hemispherical reflectance (Raman albedo) and diffuse transmittance of the powder layer to be found. The Raman gains were obtained from the ratios of transmitted and reflected fluxes with and without the pump. The contribution of the diffuse pump flux reflected from the rear boundary was included in the gain profile: $\gamma_R(\tau) = \gamma_0 \{ \exp(-\kappa_d \tau) + R_2 \exp(-\kappa_d [2\tau_0 - \tau]) \}$, where κ_d is the diffuse attenuation coefficient for the pump light, τ_0 is the total optical depth and R_2 the boundary reflectance. For thin layers,

multiple reflections at the boundaries are taken into account. For the barium nitrate powder samples used in the experiment, the inferred scattering parameters were $\lambda_s \approx 110 \mu\text{m}$ and $g \approx 0.7$, whence $\beta \approx 0.49$ and $b_1 \approx 0.4$. The Raman gain coefficient (estimated from the incident pump beam intensity) ranged from $\gamma_R = 0.5 \text{ cm}^{-1}$ to 2.2 cm^{-1} [10]. A small but positive enhancement of the Raman albedo of the powder sample at the lowest Raman gain sets a lower limit on the particle scattering albedo: $\varpi \geq 0.995$ (with an upper limit determined by the effective penetration depth). For high particle scattering albedoes ($\varpi \geq 0.995$), both pump and probe beams penetrate further into the diffusive medium, sampling relatively large gain volumes, the vector and scalar fluxes of the amplified diffuse Raman radiation reaching maximum values some 10-20 scattering lengths from the pumped surface. Thus quite modest Raman gains can result in significant amplification of the multiply scattered Raman radiation, as demonstrated by the enhanced reflectance and transmittance of barium nitrate powder [10]. Two-stream calculations of the Raman albedo A_R and Raman transmission gain T_R vs. depth L generate profiles with closely similar characteristics to those observed, except for the quasi-exponential rise for the thinner layers ($L \leq 2 \text{ mm}$) (Fig 1). However, the value of the gain parameter γ_0 required to fit the data points is lower than the experimental value as a result of the simplifications involved in the two-stream analysis, which neglects lateral diffusion of pump and probe in the finite gain volume [10].

Raman laser threshold

Increasing the Raman gain by further increasing the incident pump intensity causes the diffusely reflected flux to rise rapidly, the Raman albedo A_R diverging when the Raman gain reaches a critical value γ_c , interpreted as the threshold gain for diffusive Raman laser generation. The albedo A_R at constant gain also increases rapidly as the boundary reflectance R_b approaches the threshold for the one mirror random laser (Fig 2). The laser threshold is significantly reduced with feedback provided by external mirrors, as observed for optically pumped random lasers [15, 18]. The dependence of the Raman gain threshold on the thickness of the powder layer is shown in Fig 3 for selected values of boundary reflectance. A 100% reflector at the rear boundary significantly reduces the threshold for the thinner layers, the lowest threshold (~50% reduction) being reached when $L/\lambda_s = 20$, but its effect disappears when $L/\lambda_s > 50$. A

100% reflector situated at the pumped surface has the maximum effect[19], halving the threshold for the thick powder layers ($L > 50$ mm). The lowest threshold occurs for the thinner layers with 100% reflectors at both boundaries, where both can contribute to the feedback. Fig 4 shows the dependence of the threshold gain parameter γ_{th} on scattering asymmetry g for different pumped surface reflectances R_1 ($R_1 = 0.57$ for glass slide) with $R_2 = 1$ in each case. The full curves show $\gamma_{th} = \gamma_R \lambda_{tr}$ vs asymmetry g , the threshold increasing with transport length $\lambda_{tr} = \lambda_s/(1-g)$ as g increases. The chain curves plot $\gamma_{th} = \gamma_R \lambda_s$ vs g and show a slow decrease as g increases (constant when $R_1 = 1$). The threshold is particularly sensitive to the value of the particle scattering albedo ϖ , small changes in ϖ resulting in greater penetration depth of diffuse pump light (proportional to co-albedo $\xi = 1 - \varpi$ when $\varpi \approx 1$ and $g \Rightarrow 1$) and an increased gain path for amplified Raman radiation. The quasi-linear relation between threshold gain parameter $\gamma_R \lambda_s$ (mean gain per scattering) and co-albedo $\xi = 1 - \varpi$ is shown in Fig 5. The threshold gain parameter $\gamma_R \lambda_s$ is plotted against the diffuse attenuation parameter $\kappa_d \lambda_s$ for the pump flux in Fig 6 for the same data set, showing the monotonic increase in threshold gain with increased attenuation of the diffuse pump radiation. The full curves in Fig 5 are power law fits to the data points of the form $y = a + bx^n$, where a, b are constants and $x = \kappa_d \lambda_s$. The exponent n lies in the range $1.76 \leq n \leq 1.96$, consistent with diffusion theory ($n = 2$). Thus the threshold gain parameter scales as $\gamma_{th} \lambda_s \propto (\lambda_s/\lambda_d)^2$ where $\lambda_d = 1/\kappa_d$ is the diffusion length.

Discussion

Given the simplicity of the two-stream analysis, it is satisfying that good qualitative agreement is found between the experimental and theoretical characteristics of the Raman albedo (and by implication, with the Monte Carlo simulation). By adjusting the value of the single particle scattering albedo ϖ , the z -dependence of the pump flux profile is reproduced [10]; this value of ϖ is then used to calculate the Raman gain profiles, with appropriate re-scaling to account for the narrow forward diffraction lobe of the particle scattering pattern (phase function). As a result of the high scattering albedo ($\varpi \geq 0.995$), both pump and probe light diffuse into the depths of the powder layer, such that for the thinner layers Fresnel reflection of the diffuse flux at both boundaries has to be taken into account. An obvious refinement of the analysis would be to include the effect of the radial gain profile corresponding to the gaussian profile

of the incident pump beam, which diffuses laterally with increasing depth [10], and radial diffusion of the Raman radiation in the 'tear-drop' gain volume. In addition, we note that a gain threshold for diffusive Raman laser action in barium nitrate powder is predicted by the two-stream analysis, analogous with random laser generation via feedback scattering in random laser media [12]. The nature of laser generation in powders and its correct theoretical description is a topic of ongoing research [12, 22], such that a Raman powder laser could best be demonstrated by experiment [8]. However, the success of the non-linear two-stream model in analysing the Raman gain probe data for barium nitrate powder is encouraging and suggests it should be further tested against the experimental data for other non-linear media. The parametric dependence of the threshold for a Raman random laser is of particular interest as this tends to be model-dependent and worth testing experimentally. The reduction in gain threshold predicted for powders with near-perfect scattering, and significant reductions with reflecting boundaries, particularly at the pumped surface, augur well for low threshold Raman powder lasers. The gain threshold also decreases for particles of lower scattering asymmetry, but the required reduction in particle size results in a similar reduction in scattering length and a corresponding increase in gain threshold, such that an optimum size may be found among larger particles [20]. The quasi-exponential increase in Raman albedo with depth observed for the thinner powder layers ($L \leq 2$ mm) is not explained by the two-stream model (nor by the Monte Carlo simulation) of diffusive Raman generation, suggesting that an alternative interpretation is required for this regime, perhaps the excitation of internal resonances in individual crystallites [21] or excitation of constant flux (CF) modes in the random medium [22].

Conclusion

Two-stream analysis of the diffuse reflectance and transmittance of a Raman random gain medium gives good qualitative agreement with the experimental data for barium nitrate powder [10]. A gain threshold for diffusive Raman laser generation in a random medium is predicted on the basis of the analysis, which could be tested by experiment. The parametric dependence of the Raman laser threshold on particle scattering albedo ϖ , particle scattering asymmetry g , diffusion length λ_d and boundary reflectance R_b has been determined and the reduction in gain threshold achieved by the addition of external reflectors evaluated. The low intrinsic absorption loss (ideally

zero) associated with Raman random gain media allows order of magnitude increased penetration depths and interaction lengths compared with conventional optically pumped random lasers. As such, they allow stimulated Raman studies to be extended to mesoscopic media, as is the case for second and higher harmonic generation [2, 3].

Appendix

The diffusion equation for the scalar flux (flux density) ϕ follows on eliminating $F = F_+ - F_-$ from eqns. (1a), (1b) and writing $\phi \approx 2(F_+ + F_-)$

$$\nabla^2 \phi + S(\tau) = \kappa^2 \phi \quad (\text{A1})$$

where $\nabla^2 = d^2/d\tau^2$, $\kappa^2 = \gamma_{11}^2 - \gamma_{21}^2$ and $S(\tau)$ is the source function [18]

The coefficients γ_{11} , γ_{21} defined by eqns 3(a), 3(b) give

$$\kappa^2 = 3(1-\gamma-\varpi)(1-\gamma-\varpi g) \quad (\text{A2})$$

for the coefficient of ϕ in the diffusion equation eqn (A1). For nett gain $\gamma > 1-\varpi$, $\kappa^2 < 0$ and with $B^2 = -\kappa^2$, the diffusion equation becomes

$$\nabla^2 \phi + B^2(\tau)\phi + S(\tau) = 0 \quad (\text{A3})$$

where $B^2(\tau)$ is a diminishing function of optical depth, resulting from the decrease of Raman gain through attenuation of the pump flux viz. $\gamma_R(\tau) = \gamma_0 \exp(-\kappa_d \tau)$, where κ_d is the diffuse attenuation coefficient. In the limit $\varpi \Rightarrow 1$ (perfect scattering), $B^2 \approx 3\gamma_{tr}(\tau)$ when $\gamma_{tr} \ll 1$, and the diffusion equation for the Raman flux $\phi(\tau)$ has exact analytic solutions expressible in terms of Bessel functions [12]. When applied to diffusion in the powder layer, the flux ϕ is extrapolated to zero a distance z_e beyond the boundary, determined by the refractive index n ($z_e = 2.42$ [14, 23]). For anisotropic scattering, z_e is expressed in terms of the transport length $\lambda_{tr} = \lambda_s/(1-g)$ [23]. For a perfectly reflecting boundary z_e is infinite and the slope is set to zero: $d\phi/d\tau|_{\tau=0} = 0$. Numerical solution of eqn (A3) with these boundary conditions gives exact agreement with the two-stream analysis (which does not require extrapolation of the boundary flux).

References

1. M. A. Noginov, S. U. Egarievwe, N. Noginova, J. C. Wang H. J. Caulfield
J Opt Soc Am B **15** 2854-60 (1998)
2. S Faez P M Johnson D A Mazurenko Ad Lagendijk J Opt Soc Am B **26** 235-243 (2009)
3. S.O. Konorov, D.A. Sidorov-Biryukov, I. Bugar, J. Kova, L. Fornarini,
M. Carpanese, M. Avella, M.E. Errico, D. Chorvat Jr., J. Kova Jr., R. Fantoni,
D. Chorvat and A.M. Zheltikov Appl Phys B **78** 73-77 (2004)
4. G Zhu C E Small M A Noginov Opt Lett **33** 920-922 (2008)
5. H Fujiwara K Sasaki J Jap Appl Phys **43** L1337-L1339 (2004)
6. N M Lawandy APL **85** 5040-5042 (2004)
7. G. D. Dice, S. Mujumdar, and A. Y. Elezzabi Appl Phys Lett **86** 131105 (2005)
8. H Zhang Z Xu H Xu C Zhu Chin J Lumin **22** 66-70 (2001)
9. W Guerin N Mercadier D Brivio1 R Kaiser Opt Exp **17** 11326-11245 (2009)
10. A E Perkins, N M Lawandy Opt Commun **162** 191-194 (1999)
11. M.A. Noginov N. Noginova S. Egarievwe J.C. Wang M.R. Kokta J. Paitz
Opt Mat **11** 1-7 (1998)
12. M A Noginov, J Novak, DGrigsby and L Deych J. Opt. A: Pure Appl. Opt. **8**
S285–S295 (2006)
13. A. L. Burin H. Cao M. A. Ratner, IEEE J. Sel. Top. Quantum Electron. **9**, 124 (2003)
14. J X Zhu D J Pine D A Weitz Phys Rev A **44** 3948-3959 (1991)
15. M A Noginov G Zhu C Small J Novak Appl Phys B **84** 269-273 (2006)
16. R M Goody Y L Yung Atmospheric Radiation Pt I 2nd edn (OUP 1989)
17. A C Selden J Opt A Pure Appl Opt **2** 510-514 (2000)
18. P C de Oliveira J A McGreevy N M Lawandy Optics Letters **22** 700-702 (1997)
19. Y Feng, K Ueda Phys Rev A **68** 025803 (2003)
20. M. A. Noginov G. Zhu A. A. Frantz J. Novak S. N. Williams I. Fowlkes J Opt Soc
Am B **21** 191-200 (2004)
21. N. E Ter-Gabrie'lyan, V. M. Markushev, V. R. Belan, C. M. Briskina, O. V.
Dimitrova, V. F. Zolin A. V. Lavrov Sov. J. Quantum Electron. **21** 840–841 (1991)
22. H E Türeci Li Ge S Rotter A D Stone Science **320** 643-646 (2008)
23. R Aronson J Opt Soc Am A **12** 2532-2539 (1995)

Figure captions

Fig. 1 Raman albedo A_R and Raman transmission gain T_R of barium nitrate powder vs. thickness L of the powder layer. The theoretical curves are matched to the experimental data points \bullet , \blacksquare by adjusting the gain parameter: $\gamma_0 = 0.014$. The albedo saturates at smaller depths than the transmission gain, as observed.

Fig. 2 Dependence of Raman albedo A_R on boundary reflectance R_b for three values of Raman gain, showing a rapid rise in albedo as the boundary reflectance approaches the threshold value for a 10 mm thick powder layer.

Fig. 3 Threshold gain parameter $\gamma_R \lambda_s$ vs powder layer thickness L/λ_s expressed in units of the scattering length λ_s . The curves compare the influence of boundary reflectance on threshold gain: (a) powder layer between glass slides (b) 100% reflector at rear boundary (reflected pump flux excluded) (c) reflected pump flux included (d) 100% reflectors at both surfaces.

Fig. 4 Threshold gain parameter γ_{th} vs. scattering asymmetry g for different pumped surface reflectances R_1 ($R_1 = 0.57$ for glass slide) with $R_2 = 1$ in each case. The full curves plot $\gamma_{th} = \gamma_R \lambda_{tr}$ vs g , where the transport length $\lambda_{tr} = \lambda_s/(1-g)$. The chain curves plot $\gamma_{th} = \gamma_R \lambda_s$ vs g and show a slowly decreasing trend as g increases (constant for $R_1 = 1$).

Fig 5 Threshold gain parameter $\gamma_R \lambda_s$ vs. co-albedo $\xi = 1 - \varpi$ for different pumped surface boundary reflectances: (a) $R_1 = 0$ (b) $R_1 = 0.57$ (c) $R_1 = 0.8$ (d) $R_1 = 1$ for powder layer thickness $L = 10$ mm.

Fig 6 Threshold gain parameter $\gamma_R \lambda_s$ vs. diffuse attenuation parameter $\kappa_d \lambda_s$ for boundary reflectance $R_1 = 0, 0.57, 0.80, 1.00$, showing the monotonic increase in threshold with increasing attenuation. Power law curves with exponents n in the range $1.8 \leq n \leq 2$ provide a good fit to the calculated data points (see text).

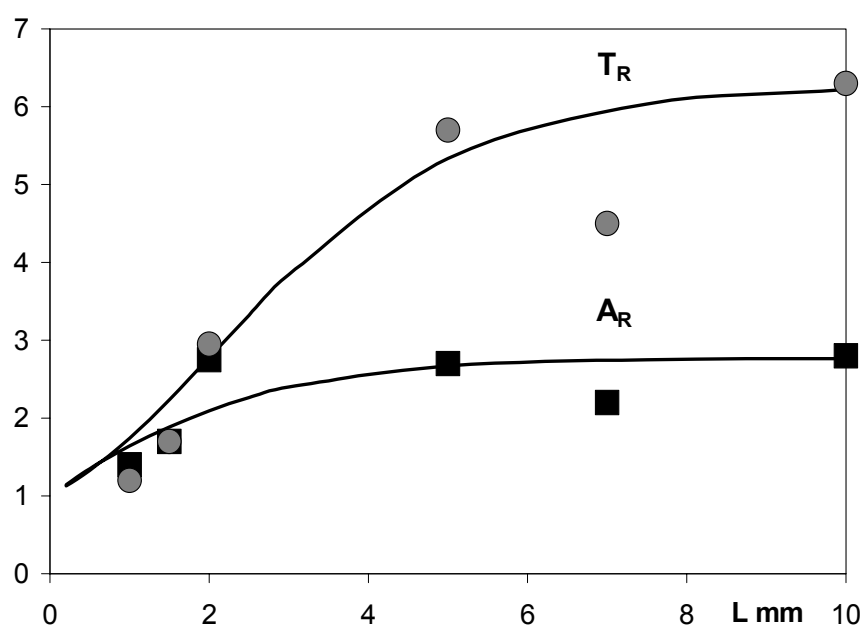


Fig 1

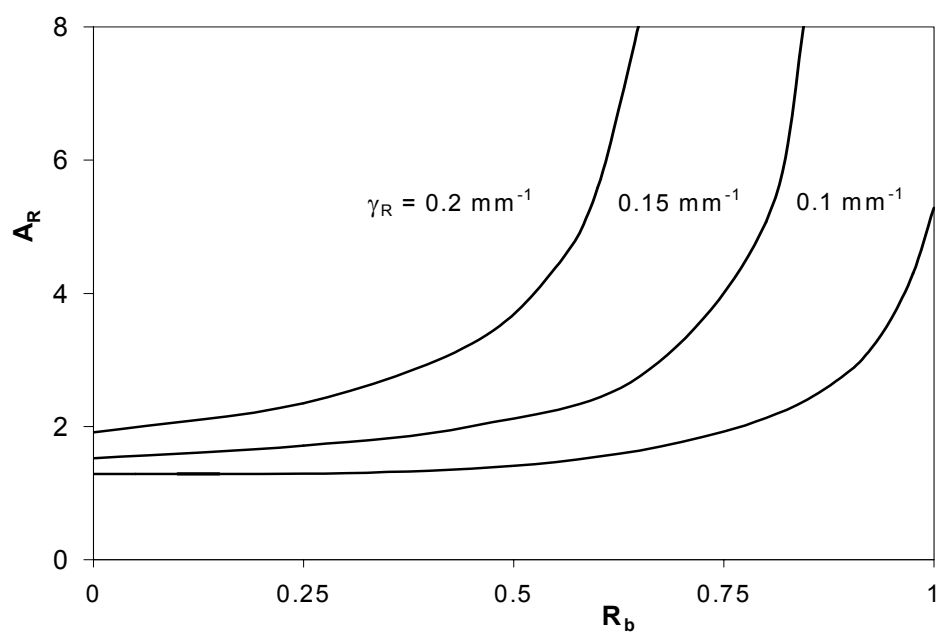


Fig 2

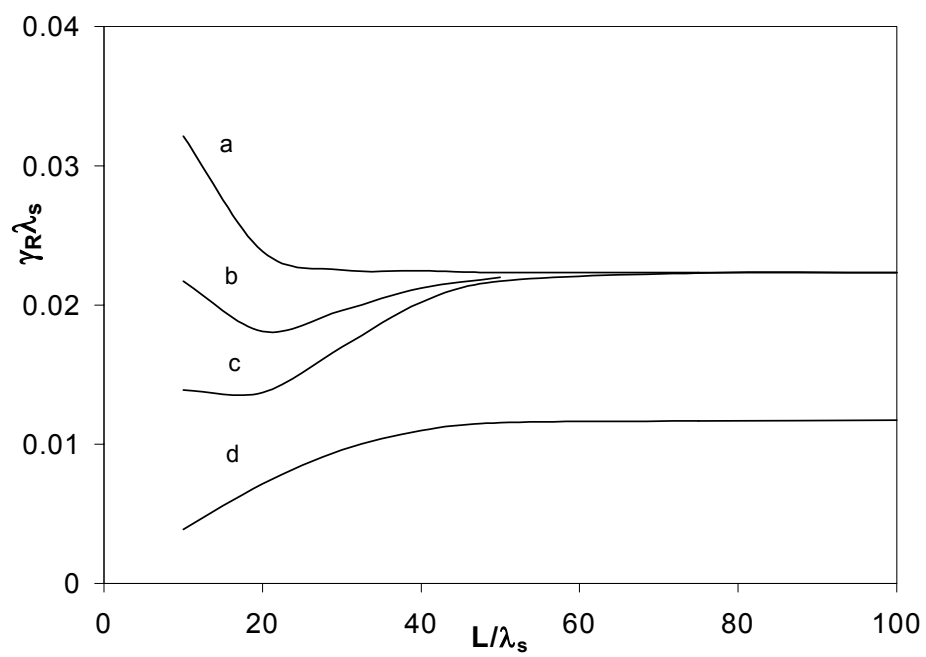


Fig 3

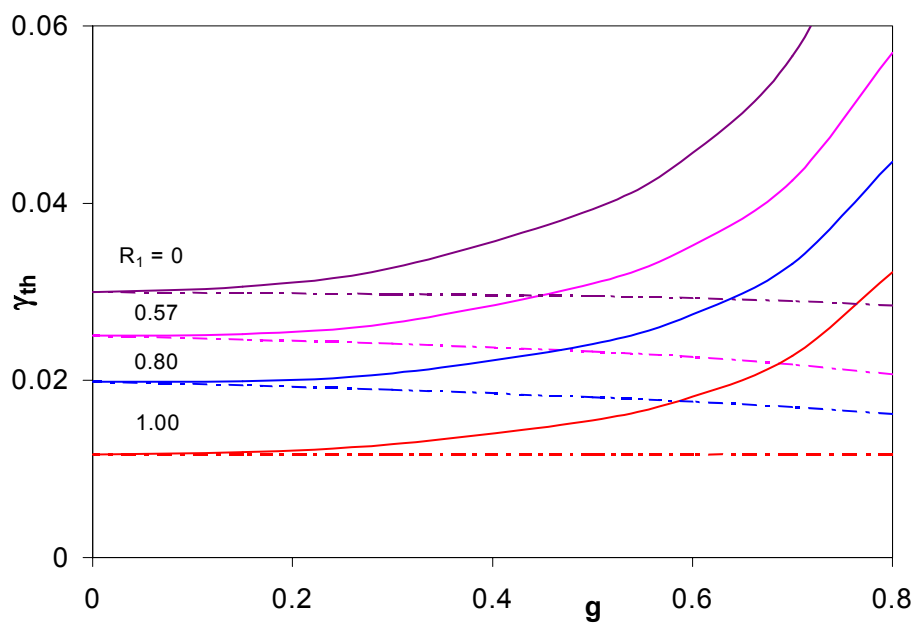


Fig 4

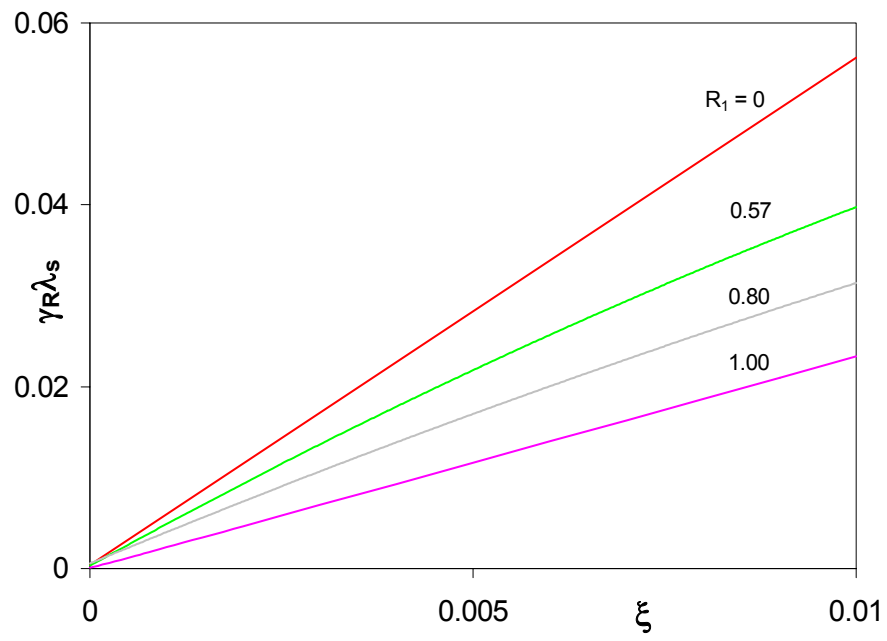


Fig 5

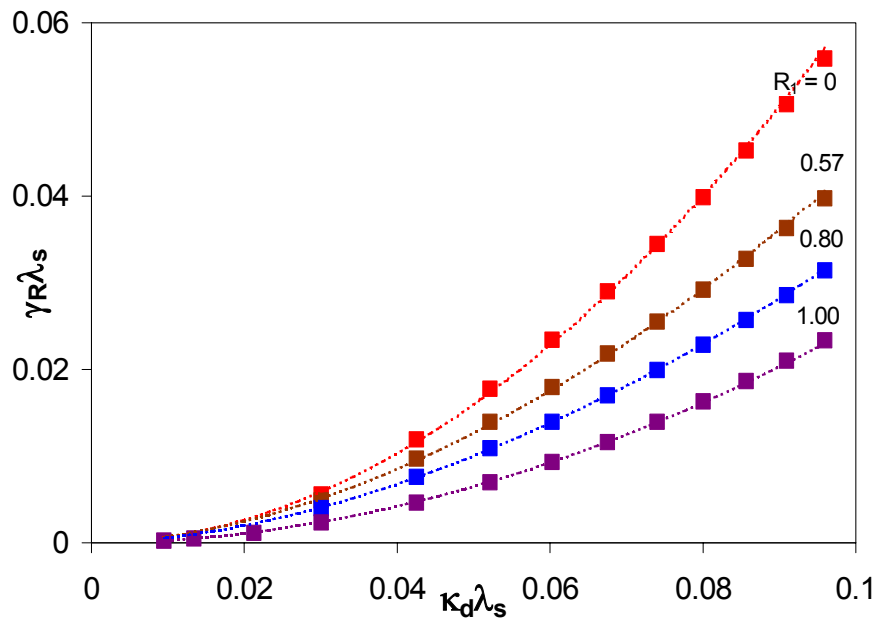


Fig 6